Shape-Memory Behavior of Thermally Stimulated Polyurethane for Medical Applications

G. Baer,[1] T. S. Wilson,[2] D. L. Matthews,[2] D. J. Maitland[2]

[1]*Department of Biomedical Engineering, University of California Davis, Davis, California 95616*
[2]*Division of Medical Physics and Biophysics, Lawrence Livermore National Laboratory, Livermore, California 94551*

Received 24 February 2006; accepted 27 September 2006
DOI 10.1002/app.25567
Published online in Wiley InterScience (www.interscience.wiley.com).

ABSTRACT: Shape memory polymers (SMPs) have been of great interest because of their ability to be thermally actuated to recover a predetermined shape. Medical applications in clot extracting devices and stents are especially promising. We investigated the thermomechanical properties of a series of Mitsubishi SMPs for potential application as medical devices. Glass transition temperatures and moduli were measured by differential scanning calorimetry and dynamic mechanical analysis. Tensile tests were performed with 20 and 100% maximum strains, at 37 and 80°C, which are respectively, body temperature and actuation temperature. Glass transitions are in a favorable range for use in the body (35–75°C), with high glassy and rubbery shear moduli in the range of 800 and 2 MPa respectively. Constrained stress–strain recovery cycles showed very low hysteresis after three cycles, which is important to know for preconditioning of the material to ensure identical properties during applications. Isothermal free recovery tests showed shape recoveries above 94% for MP5510 thermoset SMP cured at different temperatures. One material exhibited a shape fixity of 99% and a shape recovery of 85% at 80°C over one thermomechanical cycle. These polyurethanes appear particularly well suited for medical applications in deployment devices such as stents or clot extractors. J Appl Polym Sci 103: 3882–3892, 2007

Key words: polyurethanes; mechanical properties; thermal properties; glass transition

INTRODUCTION

Shape memory polymers (SMPs) represent a very interesting class of polymers, because of their ability to recover a predetermined shape upon controlled heat activation.[1] They are increasingly being investigated for use as smart materials in a variety of applications ranging from textiles to ergonomic utensils.[2] In the medical field, new SMPs with adjustable moduli, high recovery ratios, sharp and adjustable transition temperatures, and biocompatible drug-eluting surfaces have enabled their use in a variety of new applications. Specifically, SMPs are currently being researched for applications in aneurysms embolization,[3] as clot extraction devices,[4–6] and for vascular stents.[7,8] Because of their different mechanical properties above and below the glass transition temperature, the properties of heat activated SMPs can be optimized to offer both the flexibility, the resistance in compression, and the high shape recovery needed for proper insertion, positioning, deployment, and functionality of these devices. They can be deployed by a variety of heat sources: light illumination,[9,10] electric current,[11] or simple hot saline solution. In addition, their surface can readily be modified for biocompatibility and drug elution.[12,13]

Thermomechanical behavior and shape memory properties have been reported for SMP materials made from polyurethanes,[1,2,14–17] ethylene-vinyl acetate copolymers,[18] oligo(ε-caprolactones),[19] poly(ethylene glycol), and poly(ethylene terephthalates).[20] The shape memory effect of thermal SMPs resides in the structure of the polymer, which is often described as being a two phase structure comprised of a hard, or fixing phase, and a soft, or reversible phase. The hard phase consists of a dispersed glassy phase, crystallinity, or/and chemical crosslinking. The soft phase can be either amorphous or semicrystalline. Varying the amount of hard and soft phase results in significant differences in shape memory behavior, as shown by Lin and Chen's early studies with polyurethanes.[21,22] Thermomechanical properties in thin films of Mitsubishi Heavy Industry polyurethane materials have previously been investigated.[2,23,24] Their shape memory behavior was also studied when replacing and varying the amount of hard segment content.[25] These studies have shown that such materials have potential for biomedical applications, since they exhibit high

Correspondence to: T. S. Wilson (wilson97@llnl.gov).
Contract grant sponsor: U.S. Department of Energy by Lawrence Livermore National Laboratory (LLNL); contract grant number: W-7405-ENG-48.
Contract grant sponsor: National Institutes of Health/National Institute of Biomedical Imaging and Bioengineering; contract grant number: R01EB000462.
Contract grant sponsor: LLNL Directed Research and Development; contract grant number: 04-ERD-093.
Contract grant sponsor: National Science Foundation Center for Biophotonics (CBST).

strain recovery, high glass/rubber modulus ratios, and their glass transition temperatures are in a favorable range for use in the human body. Additionally, the good biocompatibility of polyurethanes is well known (e.g., catheters[26] and heart valves[27]) and has been studied for these SMPs. *In vitro* and *in vivo* studies by Metcalfe et al. of the same Mitsubishi polyurethane materials used as foams for endovascular interventions have recently shown the material to be noncytotoxic and poorly thrombogenic.[3] *In vitro* studies from our group (in the process of publication) show that the material used here has minimal effect on triggering an inflammatory response, thrombogenesis, and activation of platelets and neutrophils, reducing the risk of rejection of the implanted device. Such SMPs would appear useful for interventional medical devices, such as stents.

Other requirements of a SMP stent reside in its thermomechanical properties. The material needs to have a high shape recovery ratio when deployed at high temperature so that a small device can be inserted and navigated through the vasculature and deployed into a large device that fits the target artery. In addition, when in place at body temperature, a high modulus is desired for resistance in tension and compression. Finally, thermomechanical properties need to be stable over time. These general requirements would apply to any SMP interventional medical device.

However, results comparing the thermomechanical properties of different Mitsubishi materials of various glass transition temperatures available have not been reported. This knowledge would be extremely helpful as a base for choosing a particular material with optimal properties for a specific medical application. Additionally, it is well known that two phase systems such as segmented polyurethanes have structures that are affected by process history including shear, stress, and solvents if solution cast[1]; however, to our knowledge, the effect of cure profile on the behavior of SMPs has not been reported. It is of interest to find out to what extend varying the curing temperature might confer different properties and shape memory behavior to SMPs.

In this study, we have examined a variety of Mitsubishi polyurethanes within the scope of researching materials for stent applications. Several thermoplastic and thermoset polyurethanes with glass transition temperatures ranging from 35 to 75°C were investigated. In addition, we studied the effect of curing temperature on thermal transitions and thermomechanical properties of one of the thermosets, by having a two step curing protocol and varying the temperature of the first step. Thermal transitions were characterized by differential scanning calorimetry (DSC), dynamic mechanical properties were analyzed by dynamic mechanical analysis (DMTA), and cyclic tensile and recovery properties were examined using an MTS tensile tester. MTS experiments were performed at two temperatures relevant to a medical device functionality: 37°C (body temperature) and 80°C (actuation temperature). Previous studies reported by our group[4] have shown that temperatures of $T_g \pm 20$°C are well into the glassy and the rubbery plateau respectively. Elongation to failure, stress recovery cycles, and free recovery cycles were studied at maximum strains of 20 and 100%, which are reasonable ranges of deformation expected in medical device actuation.

EXPERIMENTAL

Materials

SMPs

The SMPs used in this study were obtained from DiAPLEX Company (a subsidiary of Mitsubishi Heavy Industries, Tokyo, Japan) either as two part thermoset resins or thermoplastic resin in pellet form. The first two digits following the two letters represent the temperature, in degree centigrade, of the first glass transition, indicated by the manufacturer. While the compositions are proprietary, it is known that the material is a segmented polyurethane, which has a microphase separated morphology.[28] The primary shape is formed at a temperature above the highest glass (T_{gh}) or crystalline (T_m) transition and the polymer is either cooled (thermoplastics) or crosslinked (thermosets) to fix the shape. The secondary shape is obtained by heating the material above the glass transition temperature of the soft phase (T_{gs}) or the soft phase crystalline melting temperature (T_{ms}), applying a strain to the material, and cooling it down below the same soft phase temperature to fix the shape. The deformation is stored elastically as macromolecular chain orientation within the soft phase, while hard phase segments are relatively imperturbed by this stress. Thus, there is an entropic potential for shape recovery. By heating the material above T_{gs} or T_{ms}, soft phase segments spring back to their lower entropic state, resulting in recovery of the primary shape.

Thermoset sample preparation

Generally, the thermoset SMPs MP3510, MP4510, and MP5510 were processed according to the sample preparation guide provided by DiAPLEX.[29] Briefly, A and B components were vacuum dried at 70°C and 1 Torr for 1 h, then mixed at the appropriate weight ratio, and degassed under vacuum (1 Torr) for 60 s. The mixture was placed into a syringe and immediately used to inject specific molds. Aluminum molds were fabricated to cast samples according to ASTM standards. DMTA samples were molded into 4.65 mm diameter, 5-cm-long cylinders; tensile test samples were molded into 1-mm-thick dogbones for failure analysis

(ASTM standard D 638 type V), and 1 mm thick, 1 cm wide bars (ASTM standard D 882) for other tensile tests. Once the molds were injected, MP5510 samples were cured in an oven under nitrogen for 1 h (cure step 1) at one of the following temperatures: 25°C (T_g − 30°C), 45°C (T_g − 10°C), 55°C (T_g) or 65°C (T_g + 10°C) followed by 4 h (cure step 2) at 80°C. MP3510 and MP4510 samples were cured in one step for 4 h at 80°C. Samples were then cooled at room temperature and stored in sealed containers before testing. DSC samples were cut from molded strips. It should be noted that the ''thermoset'' grade resins are actually comprised of difunctional monomers and when fully cured at recommended conditions were found to be soluble in appropriate solvents and melt processible. For example, heating these thermosets above the hard phase T_g would allow for re-training of the primary shape.

Thermoplastic SMP sample preparation

Test specimens were prepared from the as received thermoplastic SMP MM5510, MM4520, MM5520, MM6520, and MM7520 pellets for DSC and DMTA testing as follows. The pellets were first vacuum dried (40 mTorr, 50°C) for 120 h. They were then compression molded into plaques with dimensions 3.2 mm × 100 mm × 100 mm using a Carver hot press (200°C, 15,000 pounds, 10 min). The pressed plaques were quickly cooled by placement on an aluminum block, demolded, stored in plastic bags, and cut into 1 cm strips for testing.

Experimental procedures

Thermal and mechanical characterization of SMPs were done using the following methods.

Differential scanning calorimetry

DSC measurements were made using a Perkin–Elmer Diamond DSC equipped with an Intracooler 2, over a temperature range of −20 to 200°C using a heating rate of 20°C/min, with 5 ± 1 mg samples, consistent with ASTM D 3418. Two heating/cooling cycles were used and the T_g's from both heating cycles are reported as the average of two repeats.

Dynamic mechanical analysis

DMTA measurements were made with an ARES LS2 under dynamic oscillatory mode at a frequency of 1 Hz and initial strain of 0.01%. Testing was done under dry air, from 25 to 120°C at a linear ramp rate of 1°C/min, consistent with ASTM D 4065. For testing thermosets, test specimens were used having a cylindrical geometry of 4.65 mm diameter and 5 cm long, while torsion rectangles of 3.2 mm × 12 mm × 50 mm were used for testing thermoplastics. The shear storage modulus G', shear loss modulus G'', and the ratio of loss to storage modulus (tan δ) were plotted as a function of temperature; T_g was determined from the tan δ peak, and the glassy and rubbery moduli were read from the G' curve. In the case of the thermoplastics, first heating, first cooling, and second heating cycles were performed to capture the effect of thermal history (two repeats).

Tensile

Stress–strain measurements were performed on an MTS Synergie 1000 tensile tester with a load cell of 5 kN, equipped with a custom forced air heating and a cooling system and a constant temperature chamber to which was attached a thermocouple. Tests were performed at 37 and 80°C after heating the sample at a rate of 10°C/min, and maintaining the sample at the desired temperature for 5 min before performing the experiment. Uniaxial elongation to failure tests were conducted at an engineering strain rate of 0.5 min^{-1}, as specified in ASTM D882. Initial modulus, peak load, peak stress, and strain at break were recorded for various thermosets with three repeats each.

Constrained stress recovery

Constrained stress recovery cycles at high temperature were conducted on the MTS Synergue 1000 at a constant strain rate of 5 min^{-1} with maximum strains of 20 and 100% and at constant temperatures of 80°C, according to the same heating protocol mentioned earlier. The machine was programmed to perform cycles of elongation to the maximum desired strain and return back to zero strain. Percentage recovery strain was calculated for each cycle. Five cycles were performed on various thermosets with three repeats.

Isothermal free recovery

Free isothermal recovery tests at high temperature were performed on the MTS Synergie 1000 as in constrained recovery cycles, except that after elongation to a maximum strain, unloading was done by programming the machine to return to a very low stress value close to 0. The sample was allowed to freely recover its strain for 15 min before the next cycle. Percentage strain recovery was then calculated. Various thermosets were tested with three repeats each.

Thermomechanical cycling

Thermomechanical cycling tests were conducted on the MTS Synergie 1000 at a constant strain rate of

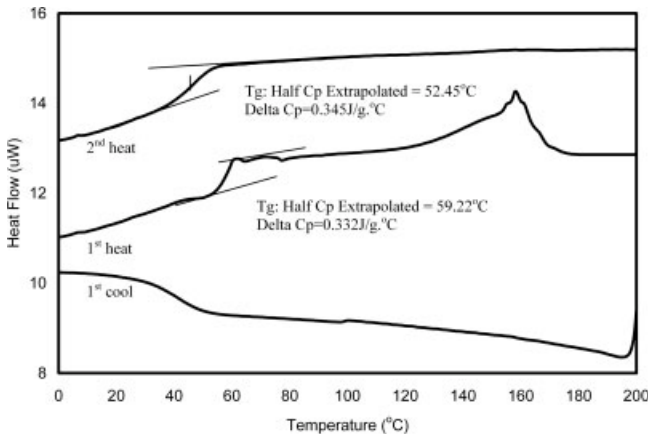

Figure 1 General DSC behavior of thermoplastic and thermoset polyurethane SMPs. Shown are first heating, first cooling, and second heating curves.

5 min^{-1} with maximum strains of 20 and 100% with elongation at a constant temperature of 80°C and subsequent cooling and recovery at 37°C, as described by Kim et al.[14] Heating was performed according to the protocol mentioned earlier. The specimen was then elongated to the desired strain, held, and rapidly cooled down to 25°C using nitrogen gas. After holding the sample at this temperature for 5 min, the stress was set to a low value close to 0, and the sample was then allowed to freely recover to its recovery strain by rapid heating at 80°C. Percentage shape fixity and Percentage shape recovery were calculated. One cycle was performed with one of the thermoset materials, with three repeats.

RESULTS AND DISCUSSION

Differential scanning calorimetry

The glass transition of the soft phase (T_g) was calculated from first and second heating curves generated by DSC using the half-height technique as described by Wunderlich[30] and as shown in Figure 1. Results for the thermoset and the thermoplastic series are shown in Table I. Also shown are results for the MP5510 thermoset series (manufacturer reported T_g of 55°C) prepared at different precuring temperatures. In general, the glass transition temperatures measured by DSC were lower than the ones indicated by the manufacturer, by up to 10°C. Since we have no specific information on the characterization method used by the manufacturer, we can only speculate on the source of this difference. The glass transition is a dynamic property and therefore varies with the cooling and heating rates of the samples. In addition, DSC and DMTA measurements often give different results; e.g., the T_g measured by DSC is often much lower than that determined by the tan δ peak,[31] which is discussed later. There was also a significant difference between the glass transition temperature obtained during the first and second heat, indicative of the importance of previous process history on phase separation and quenching of the amorphous soft phase. Surprisingly, cure step 1 temperature did not affect the glass transition temperature significantly.

Dynamic mechanical analysis

Results of the DMTA testing are shown in Figures 2 through 3. Glass transitions were determined based on tan δ peak and are reported in Table I. Figure 2(a) shows the shear storage modulus G' and tan δ for the different T_g grade thermoset SMPs prepared according to manufacturer's recommendations with one step curing. Figure 2(b) shows G' and tan δ for thermoplastic SMP MM-5510 during first heating, first cooling, and second heating. The effect of thermal history is captured here. There is a shift in the curves between first heating and first cooling. The first cooling and the second heating display identical curves. Between the first heating and first cooling, there is a

TABLE I
Summary of DSC and DMTA Results on DiAPLEX® (Mitsubishi) SMPs and Comparison with Manufacturer's Values

SMP type	Cure step 1 conditions	Cure step 2 conditions	Manufacturer's soft phase T_g (°C)	T_g by DSC first heat (°C)	T_g by DSC second heat (°C)	T_g by tan δ (°C)	Glassy plateau modulus (Pa)	Rubbery plateau modulus (Pa)
MP3510	–	4 h 80°C	35	31.3	25.2	46.1	5.2 E 8	1.6 E 6
MP4510	–	4 h 80°C	45	42.5	35.9	54.1	7.0 E 8	1.7 E 6
MP5510	–	4 h 80°C	55	52.4	51.1	65.2	8.1 E 8	1.9 E 6
MM5510	–	10 min 200°C	55	51.4	52.0	54.9	8.1 E 8	1.6 E 6
MM4520	–	10 min 200°C	45	35.9	47.2	45.9	6.6 E 8	1.3 E 6
MM5520	–	10 min 200°C	55	45.9	53.5	57.3	7.7 E 8	1.4 E 6
MM6520	–	10 min 200°C	65	64.7	64.9	66.6	8.9 E 8	2.1 E 6
MM7520	–	10 min 200°C	75	74.2	74.4	74.6	7.7 E 8	1.8 E 6
MP5510	1 h 25°C	4 h 80°C	55	44.3	52.4	55.9	7.9 E 8	1.5 E 7
MP5510	1 h 45°C	4 h 80°C	55	43.3	51.0	61.3	8.3 E 8	5.9 E 6
MP5510	1 h 55°C	4 h 80°C	55	41.7	55.2	65.4	7.6 E 8	2.5 E 6
MP5510	1 h 65°C	4 h 80°C	55	44.5	52.6	66.3	7.7 E 8	2.1 E 6

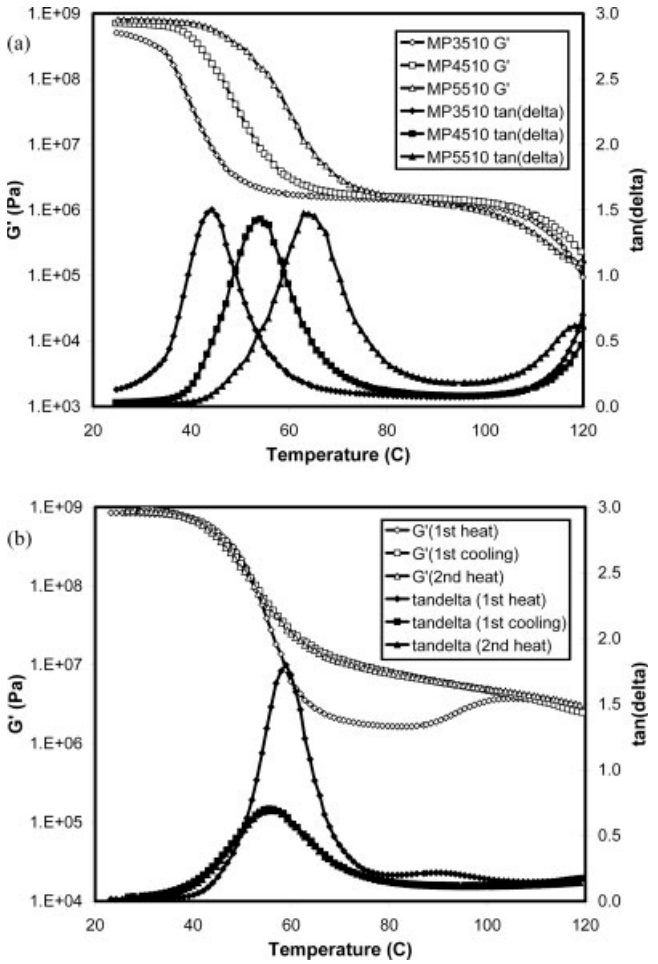

Figure 2 Elastic modulus and tan δ of SMPs. (a) Thermosets cured using suggested temperature profile and (b) first heating, first cooling, and second heating cycles for the MM5510 thermoplastics.

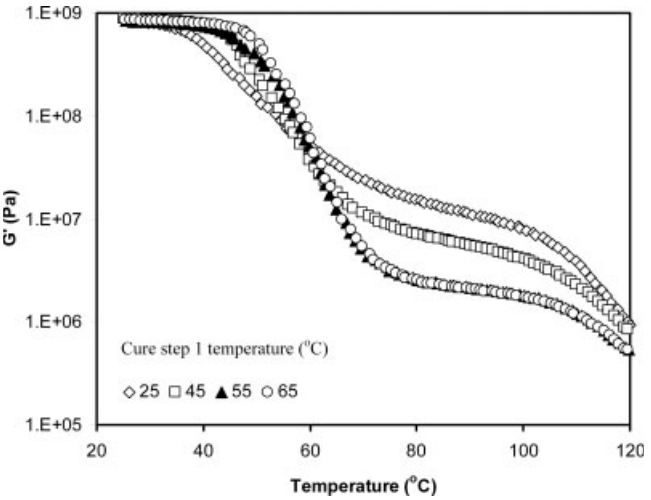

Figure 3 Dynamic storage modulus (G') in the first heat for MP5510 SMP cured at various cure step 1 temperatures.

shift to lower T_g. There is also a decrease in tan δ peak height, indicating an increase in the hard phase content. In addition, the storage modulus in the glassy phase increases by a factor of 8 between the first heating and the first cooling. These results can be understood as a rearrangement in the phase-separated structure of the polymer as a result of thermal history during testing. Initially, during preparation, the test specimens were quickly cooled from the melt and the segregation of soft phase segments and hard phase segments into separate phases did not have time to reach equilibrium. The result would be a structure made up of soft phase containing a relatively high hard-segment content. The results from the first heating cycle are indicative of this structure up to the point at which the polymer had enough mobility to regain an equilibrium phase structure. On cooling and subsequent reheating, the polymer has had time to reach this equilibrated structure in which a higher degree of phase separation has occurred, with the result that the soft phase now has a lower hard segment content (hence lower T_g) and there is a larger amount of hard phase (hence higher modulus). It is likely that more cycling would show identical curves.

Cure temperature effects can also be seen in the thermoset grade SMPs as seen in Figure 3, which shows G' obtained with the MP5510 thermoset materials cured in two steps. Glass transitions were determined based on tan δ peak. The glassy and rubbery moduli can also be read; they are two elastic moduli of importance, which are approximately equal to the shear storage modulus G' in the lower temperature higher stiffness ''glassy'' plateau and in the higher temperature lower stiffness ''rubber'' plateau, respectively. For SMPs, the rubbery and the glassy moduli are generally taken as the elastic moduli at $T_g \pm 25°C$, respectively. Results are shown in Table I. Overall, glass transition temperatures obtained by tan δ peak

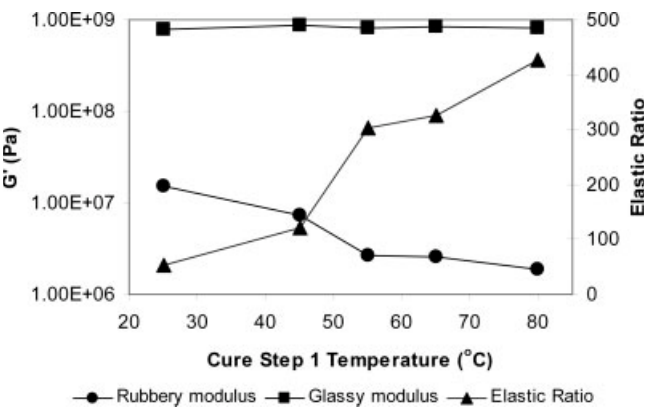

Figure 4 Glassy (G' at $T_g + 25°C$), rubbery (G' at $T_g - 25°C$) modulus, and Elastic ratio (G' at $T_g - 25°C$/G' at $T_g + 25°C$) versus cure step 1 temperature for the thermoset polymers MP5510.

TABLE II
Glass Transition Temperatures, Modulus, and Elastic Ratio for the MP5510 Thermoset Series Cured at Various Temperatures in One or Two Steps

Cure step 1 temperature (1 h) (°C)	Cure step 2 conditions (4 h) (°C)	T_g from tan δ peak (°C)	G' at $T_g + 25$ Pa	G' at $T_g - 25$ Pa	Elastic ratio
25	80	55.9	1.5 E +07	7.9 E +08	53
45	80	61.3	7.2 E +06	8.7 E +08	121
55	80	65.4	2.7 E +06	7.6 E +08	304
65	80	66.3	2.6 E +06	8.2 E +08	327
–	80	65.2	1.9 E +06	8.5 E +08	426

were higher than the ones obtained by DSC. This is very common; T_g in DSC is taken at one half of the increase in heat capacity, while T_g taken at the tan δ peak occurs after the shear loss modulus G'' has peaked, thus further into the glass transition and at a higher temperature.[30] For the thermoplastic series, T_g measured by tan δ was close to the manufacturer's T_g. For the thermoset series cured in two steps, the T_g measured by tan δ varied between 61.3 and 66.3°C. The glassy shear modulus was roughly constant across all materials, in the order of 800 MPa. The rubbery shear modulus seemed to be slightly more elevated in the thermoset materials when compared to the thermoplastic materials, and overall varied between 1.3 and 15 MPa, generally increasing with increasing T_g. However, for the MP5510 thermosets cured in a two-step process, while the glassy modulus remained essentially unchanged, the rubbery modulus significantly decreased with increasing precuring temperature, reaching a plateau for materials cured above 55°C during cure step 1, as seen in Figures 3 and 4.

The elastic ratio, defined as the ratio of the glassy to rubbery modulus ($G'(T_g - 25°C)/G'(T_g + 25°C)$), increased with increasing temperature during cure step 1 of the thermoset series, as shown in Table II and Figure 4. It has been reported that a high glassy modulus correlates with high shape fixity during simultaneous cooling and unloading, and elasticity ratios above 100 allow for greater resistance to deformation and better shape recovery.[13] According to these findings, material with cure step 1 at 25°C should exhibit less shape recovery than the others, since the elastic ratio is 53 while other elastic ratios are above 100.

The increase in the elastic ratio, due to a decrease in the rubbery modulus, could be explained by an increase in phase separation of the material, as the temperature is increased during cure step 1.[14] Visual observations of the turbidity of the samples cured at the different temperatures appear to support this idea. It was observed that in general, the degree of turbidity in the samples increased with initial (step 1) cure temperature. Samples cured at 25 and 45°C in cure step 1 showed little turbidity and were almost transparent, while the ones cured at 55 and 65°C in cure step 1, and the ones cured at 80°C in one single step, showed increasing degrees of turbidity. Higher turbidity seemed to correlate with lower rubbery modulus. Turbidity or cloudiness occurs in multiphase systems because of the differences in the refractive indices between phases, in turn relating to different compositions, the presence of additives or dispersed fillers, or crystallinity. Here we believe increases in turbidity are related to the degree of phase separation and/or changes in size of the dispersed phase.

MTS mechanical testing

Uniaxial tensile test to failure—MTS (37 and 80°C)

Figure 5 shows the stress–strain behavior during uniaxial tensile testing to failure at 37 and 80°C. At a given temperature test, the materials exhibited very similar curves, with quite different strains at break. The maximum strain at break was 100% at 37°C and 270% at 80°C. The material exhibited necking at 37°C, but not at 80°C. This is presumably due to cross section contraction with realignment of the polymer chains along the extension direction.[14] Table III shows failure test results at 37 and 80°C. The strain at break at 37°C was highest for the material precured at 25°C and decreased with increasing precuring temperature, suggesting a lower degree of phase separation as curing

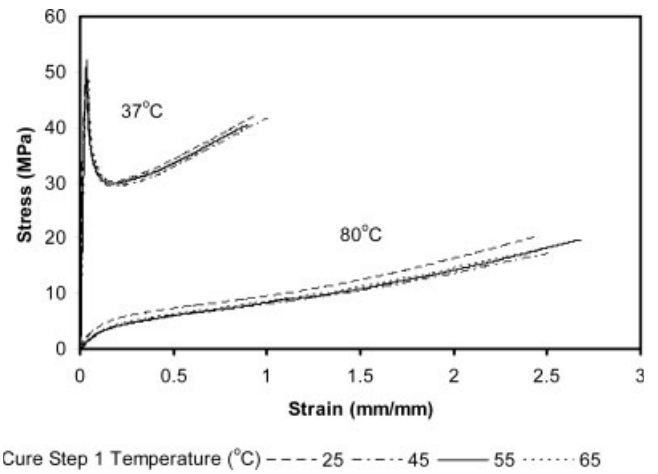

Figure 5 MP5510 thermoset series tensile testing to failure.

TABLE III
Tensile Testing Results for the MP5510 Thermoset Series

Specimen					
Cure step 1 temperature (°C)	Test temperature (°C)	Peak load (N)	Peak stress (MPa)	Strain at break (%)	Initial modulus (MPa)
25	37	142 ± 1	46 ± 1	95 ± 5	1943 ± 16
45	37	149 ± 1	48 ± 1	88 ± 8	1962 ± 35
55	37	158 ± 1	51 ± 1	71 ± 8	2027 ± 18
65	37	153 ± 1	49 ± 1	51 ± 3	1966 ± 16
25	80	68 ± 4	22 ± 2	263 ± 12	35 ± 2
45	80	51 ± 4	16 ± 2	245 ± 3	26 ± 1
55	80	60 ± 4	19 ± 2	271 ± 8	23 ± 1
65	80	53 ± 4	17 ± 2	241 ± 8	27 ± 1

temperature increases.[14] Strain at break at 80°C was highest in the material precured at 55°C. Peak prestresses were similar across materials at a given test temperature, around 50 MPa at 37°C, and 19 MPa at 80°C.

Isothermal constrained stress recovery cycles

Cyclic behavior at 80°C and 20% maximum strain. All isothermal constrained stress recovery cycles showed a hysteresis, which decreased with increasing cycle number. Figure 6 shows the stress–strain cyclic behavior for the material precured at 25°C. As seen in this figure, the greatest change in behavior is observed between the first and the second cycle. This is presumably due to entanglement decoupling of molecular chains, with relaxation of dangling chains and pulling out of hard segments from the hard phase. Cyclic properties become similar after the third cycle. This is important to know in terms of manufacturing and preconditioning the material to create a device with uniform cyclic properties. In addition, as the number of cycles increases, the initial slope of the loading curve does not significantly change, which implies that the structure is unchanging. These results are similar to the ones reported by Tobushi et al.[2] This stress–strain behavior was observed in all the precured conditions studied. Figure 7(a,b) shows the first and the fifth cycle for materials precured at 25, 45, 55, and 65°C. The material precured at 25°C clearly exhibits higher stresses at 20% strain when compared to the other materials, which exhibit identical behavior. The material precured at 25°C also had the largest initial slope, suggesting it has higher resistance to deformation among these materials. This suggests the existence of a transition precuring temperature between 25 and 45°C below which more phase separation occurs during preparation of the material.

Cyclic behavior at 80°C and 100% maximum strain. Figure 8 shows the stress–strain cyclic behavior for the material

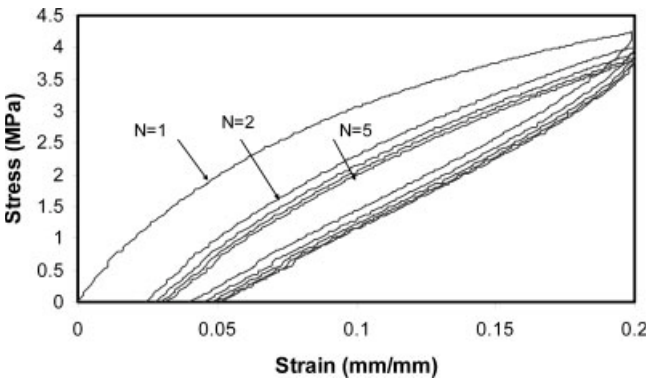

Figure 6 Constrained isothermal stress recovery cycles at 80°C for the material cured for 1 h at 55°C followed by 4 h at 80°C. Maximum strain 20%.

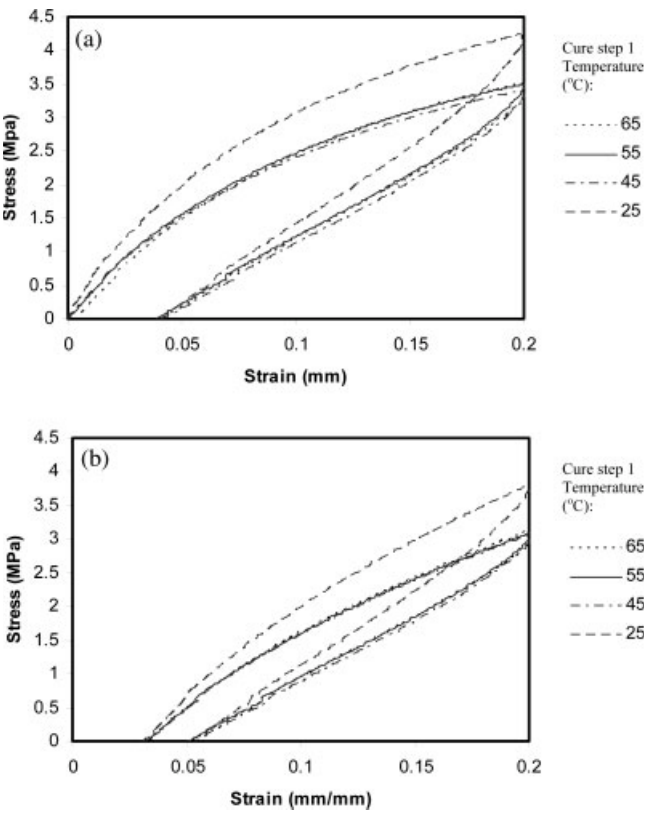

Figure 7 MP5510 thermoset series: constrained isothermal strain recovery at 80°C, (a) cycle 1 and (b) cycle 5.

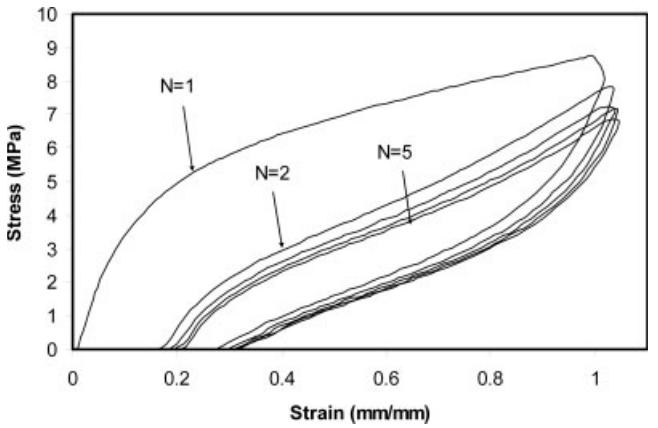

Figure 8 Constrained isothermal stress recovery cycles at 80°C for the material cured at 55°C for 1 h followed by 4 h at 80°C. Maximum strain 100%.

precured at 55°C. As in the curves obtained at 20% maximum strain, the greatest change in behavior occurs between the first and the second cycle. Unlike in the 20% maximum strain curves, however, a yield point is present but is more prominent in the first cycle. The initial slope decreases with increasing cycles, suggesting that the resistance to deformation decreases with the number of cycles. This is presumably due to microscopic rearrangement of hard segments during extension to 100% strain, occurring mostly during the first cycle, as previously described by Kim et al.[14] This rearrangement is also seen as an increase in the slope after the yield point with increasing cycle number. Cyclic properties become similar after the third cycle. This stress–strain behavior was observed in all the materials studied. Figure 9(a,b) show the first and the fifth cycle for materials precured at 25, 45, 55, and 65°C. The clear difference in stresses between the material precured at 25°C and the other materials seen in the 20% maximum strain deformation experiments is not as pronounced here, but the material precured at 20°C exhibits the highest resistance to deformation here again.

The percentage strain recovery was calculated as follows

$$R_r = [(\varepsilon_m - \varepsilon_p)/\varepsilon_m]100,$$

where ε_m is the maximum strain at maximum stress, and ε_p is the residual strain after recovery, i.e., the strain at the beginning of the next cycle. Figure 10 shows the percentage strain recovery obtained in the different precuring conditions as a function of cycle number. As expected, the percentage strain recovery is higher for a maximum elongation of 20% (88% for the first cycle) than for a maximum elongation of 100% (84% after the first cycle) but they seem to follow the same trend and remain parallel to each other, with the largest decrease between the first and the second cycle. However, this commonly used calculation does not reflect the fact that the next cycle does not start at zero strain, which means that the percentage recovery actually increases with cycle number. To appreciate this, the adjusted recovery strain can be calculated as follows for each cycle

$$R_{r\,\mathrm{adj}} = [(\varepsilon_m - \varepsilon_p)/(\varepsilon_m - \varepsilon_0)]100$$

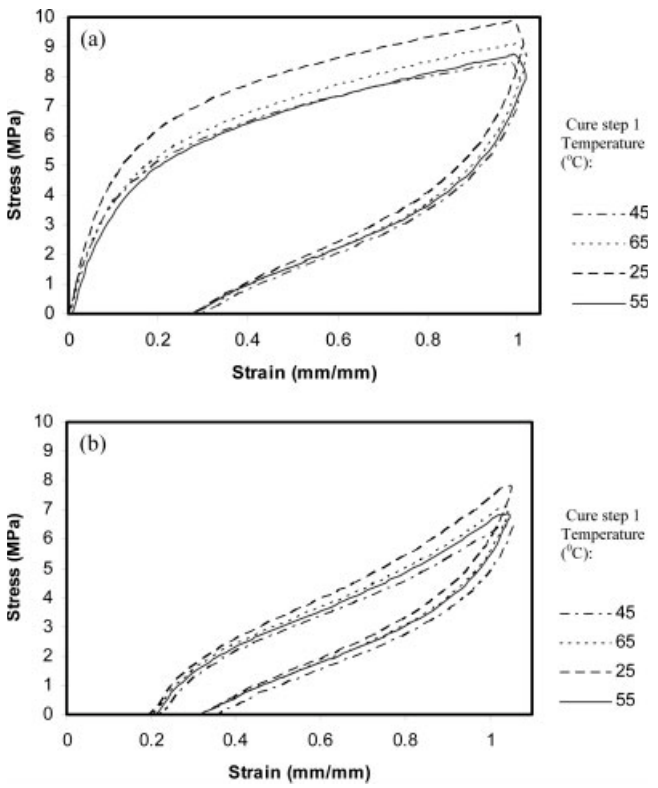

Figure 9 MP5510 thermoset series: constrained isothermal strain recovery at 80°C, (a) cycle 1 and (b) cycle 5.

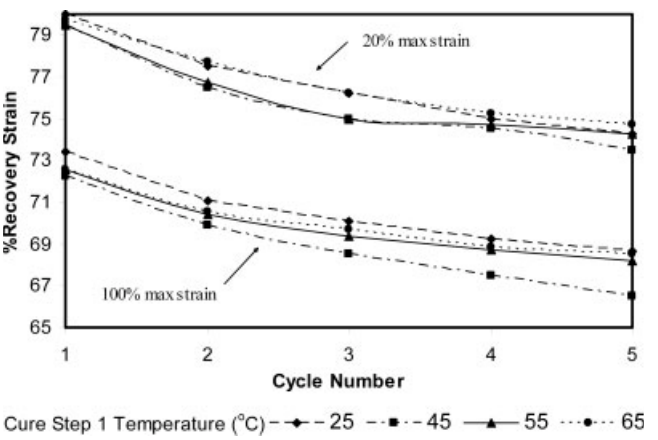

Figure 10 Percentage recovery strain (constrained) at 80°C as a function of cycle number.

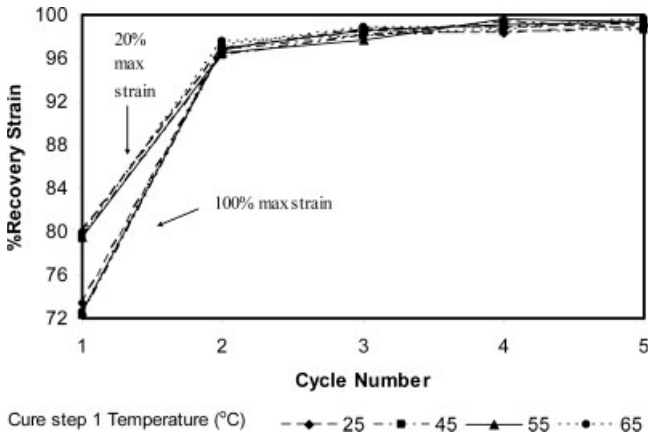

Figure 11 Adjusted percentage recovery strain (constrained) at 80°C as a function of cycle number.

where ε_m is the maximum strain, ε_p is the residual strain after recovery, and ε_0 is the strain at the beginning of the cycle. Note that ε_0 of cycle 1 is 0, and ε_0 of cycle N corresponds to ε_p of cycle $N - 1$. Figure 11 shows the adjusted recovery strain as a function of cycle number. After the second cycle, 97% strain recovery is obtained for both 20 and 100% maximum strain tests. Over 99% recovery is obtained after the fifth cycle. This shows that preconditioning samples by five cycles of elongation should result in constant deformation properties. It is important to note that these tests were performed in constrained recovery. Thus, the material has even more potential for shape recovery, if more time is allowed for it to recover, as in free recovery tests.

Free isothermal recovery tests

Free isothermal recovery tests were performed on the MTS. The specimens were elongated to a maximum strain of 20% in the chamber at 80°C, and then allowed to freely return to their initial strain for 10 min, at the same temperature. For this, the stress was set to a very small value. Stress and strain were recorded continuously. The various MP5510 thermosets were tested, and recovery strains above 90% were obtained, with no significant difference between materials, as seen on Table IV. Note that the method we used for evaluating the free recovery strain is limited by the resolution of the load cell. In addition, the PDI control settings introduce some oscillations, which also introduce errors. These oscillations were so prominent during testing at 100% maximum strain that data could not be analyzed. A better method would be to measure free recovery by videotaping.

TABLE IV
Percentage Strain Recovery of MP5510 Thermosets Obtained in the Free Recovery Tests Performed at 80°C with Maximum Elongation of 20%

Cure step 1 temperature (°C)	Strain recovery (%)
25	94 ± 1
45	94 ± 1
55	96 ± 2
65	95 ± 2

Thermomechanical cycles

Samples precured at 55°C were run through one cycle of shape fixing and recovery experiments, as described in the previous section. The sample was elongated to a maximum strain ε_m at 80°C, the shape was then fixed by rapid cooling at 25°C using compressed air, and the load was removed. Because of contraction of the material during cooling, the new strain at zero stress ε_u was lower than ε_m. The material was then heated at 80°C or at 37°C and allowed to recover its shape for 10 min back to ε_p. The percentage shape recovery and the percentage shape

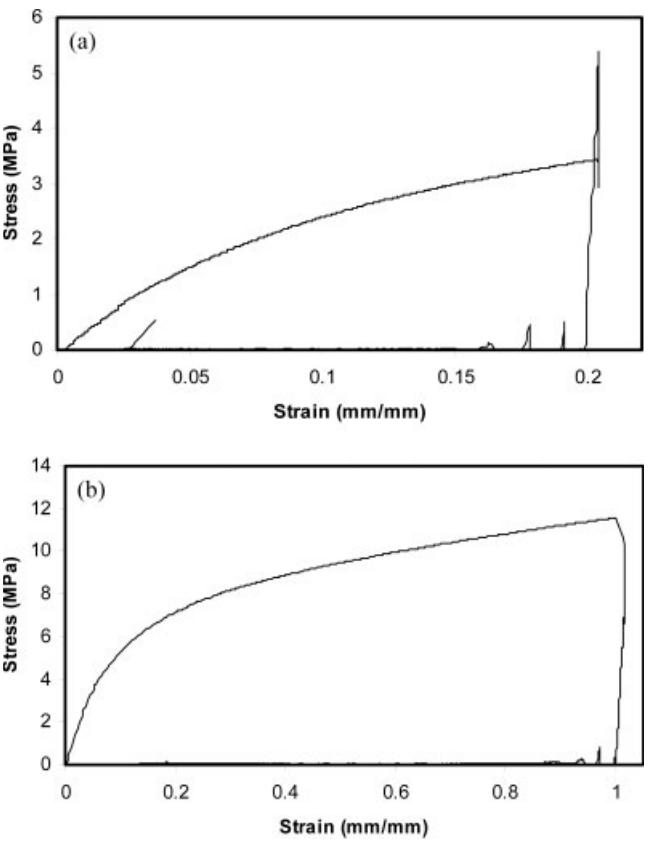

Figure 12 Thermomechanical cycling curves at 80°C for MP5510 thermoset material cured at 55°C for 1 h, followed by 4 h at 80°C. (a) Maximum 20% strain and (b) maximum 100% strain.

TABLE V
Shape Fixity and Shape Recovery Obtained after One Thermomechanical Cycle of MP5510 Thermoset Material Cured at 55°C for 1 h, Followed by 4 h at 80°C

Recovery temperature (°C)	ε_m	ε_p	ε_u	Percentage shape fixity	Percentage shape recovery
37	0.2	0.168 ± 0.001	0.192 ± 0.001	96.3 ± 0.4	16.0 ± 0.4
80	0.2	0.024 ± 0.007	0.195 ± 0.003	98.5 ± 1.4	89.5 ± 3.5
37	1	0.930 ± 0.010	0.993 ± 0.003	99.3 ± 0.3	5.5 ± 1.1
80	1	0.142 ± 0.001	0.991 ± 0.001	99.5 ± 0.1	84.6 ± 1.6

fixity were calculated as follows

$$\% \text{ shape fixity} = (\varepsilon_u/\varepsilon_m)100$$

$$\% \text{ shape recovery} = [(\varepsilon_m - \varepsilon_p)/\varepsilon_m]100$$

Figures 12(a,b) show plots of stress versus strain for the MP5510 thermoset material precured at 55°C, elongated to 20% [Fig. 12(a)] or 100% [Fig. 12(b)] maximum strain, cooled at 25°C, and heated at a recovery temperature of 80°C. The high shape fixity both at 20 and 100% maximum strain is evident from these curves. Table V shows shape fixity and shape recovery obtained at the various maximum strains and recovery temperatures for this material. The average shape recovery at a recovery temperature of 80°C was 87%, which is less than the values obtained for recovered samples in the free recovery experiments. This most likely reflects the influence of fixing the shape on the recovery ratio. Recovery at 37°C was in the order of 10%; this is expected, since this temperature is well below the glass transition temperature of the soft phase. Very high percentage shape fixity between 96 and 99.5% were obtained.

CONCLUSIONS

We have studied the thermomechanical properties of commercial thermoplastic and thermoset polyurethanes of various compositions for medical applications. Their glass transition temperatures measured by DMTA and DSC varied between 45 and 75°C. The average glassy modulus was 700 MPa, and the average rubbery modulus was in the order of 1.8 MPa. The glassy modulus was fairly constant across the materials, but there were significant variations in the rubbery modulus between the thermosets cured at different temperatures, and in thermoplastics, as a function of cooling rate during processing. Sample turbidity and prior works suggest these effects are due to differences in microphase structure. This shows that it is possible to manipulate the elastic ratio by changing curing conditions, to obtain different desired recovery properties. Stress–strain relationships were studied at relevant temperatures for medical interventional devices: body temperature of 37°C (expanded device) and actuation temperature of 80°C, at relevant strains of 20 and 100%. Failure strains of 100 and 250% were achieved at 37 and 80°C respectively. Constrained recovery cycles showed a similar behavior after cycle 5, suggesting that preconditioning is an important consideration for these materials. Finally, thermocycles showed shape recovery over 85% and shape fixity up to 99%. Thus, thermomechanical properties of these materials can be adjusted and seem to be well suited for manufacturing medical interventional devices such as thromboembolic extractors and vascular stents.

CBST, an NSF Science and Technology Center, is managed by the University of California, Davis, under Cooperative Agreement No. PHY 0120999.

References

1. Landlein, A.; Kelch, S. Angew Chem Int Ed Engl 2002, 41, 2034.
2. Tobushi, H.; Hara, H.; Yamada, E.; Hayashi, S. Smart Mater Struct 1996, 5, 483.
3. Metcalfe, A.; Desfaits, A.-C.; Salazkin, I.; Yahia, L. H.; Sokolowski, W. M.; Raymond, J. Biomaterials 2003, 24, 491.
4. Metzger, M.; Wilson, T. S.; Schumann, D. L.; Matthews, D. L.; Maitland, D. J. Biomed Microdevices 2002, 4, 89.
5. Small, W.; Wilson, T.; Benett, W.; Loge, J.; Maitland, D. J. Opt Express 2005, 13, 8204.
6. Small, W.; Metzger, M.; Wilson, T.; Maitland, D. J. IEEE J Selected Topics Quantum Electron 2005, 11, 892.
7. Wache, H. M.; Tartakowska, D. J.; Hentrich, A.; Wagner, M. H. J Mater Sci Mater Med 2003, 14, 109.
8. Gall, K.; Yakacki, C. M.; Liu, Y.; Shandas, R.; Willett, N.; Anseth, K. S. J Biomed Mater Res A 2005, 73, 339.
9. Maitland, D. J.; Metzger, M.; Schumann, D. L.; Lee, A.; Wilson, T. S. Lasers Surg Med 2002, 30, 1.
10. Lendlein, A.; Jiang, H.; Junger, O.; Langer, R. Nature 2005, 434, 879.
11. Hilmar, K.; Price, G.; Pearce, N.; Alexander, M.; Vaia, R. A. Nat Mater 2004, 3, 115.
12. Landlein, A.; Langer, R. Science 2002, 296, 1673.
13. Bertmer, M.; Buda, A.; Blomenkamp-Hofges, I.; Kelch, S.; Lendlein, A. Macromolecules 2005, 38, 3793.
14. Kim, B. K.; Lee, S. Y.; Xu, M. Polymer 1996, 37, 5781.
15. Li, F.; Zhang, X.; Hou, J.; Xu, M.; Luo, X.; Ma, D.; Kim, B. K. J Appl Polym Sci 1997, 64, 1511.
16. Park, H.; Kim, J. W.; Lee, S. H.; Kim, B. K. J Macromol Sci Part B: Phys 2004, 43, 2, 447.

17. Hayashi, S.; Shunichi, E. U.S. Pat. 5,145,935 (1992).
18. Li, F.; Zhu, W.; Zhang, X.; Zhao, C.; Xu, M. J Appl Polym Sci 1999, 71, 1063.
19. Lendlein, A.; Schmidt, A. M.; Schroeter, M.; Langer, R. J Polym Sci Part A: Polym Chem 2005, 43, 1369.
20. Park, C.; Lee, J. Y.; Chun, B. C.; Chung, Y.-C.; Cho, J. W.; Cho, B. G. J Appl Polym Sci 2004, 94, 308.
21. Lin, J. R.; Chen, L. W. J Appl Polym Sci 1998, 69, 1563.
22. Lin, J. R.; Chen, L. W. J Appl Polym Sci 1998, 69, 1575.
23. Ju, J. L.; Ji, F. L.; Wong, Y. W. Polym Int 2005, 54, 600.
24. Tobushi, H.; Matsui, R.; Takada, T.; Hayashi, S. Presented at the XXI ICTAM, Warsaw, Poland, August 15–21, 2004.
25. Yang, J. H.; Chun, B. C.; Chung, Y.-C.; Cho, J. H. Polymer 2003, 44, 3251.
26. Lamba, N. M. K.; Woodhouse, K. A.; Cooper, S. L. Polyurethanes in Biomedical Applications; CRC Press: New York, 1997.
27. Butterfield, M.; Wheatley, D. J.; Williams, D. F.; Fisher, J. J Heart Valve Dis 2001, 10, 105.
28. Hayashi, S. Int Prog Urethanes 1993, 6, 90.
29. Mitsubishi Heavy Industries. Processing Instructions for Mitsubishi Shape Memory Polymer, Manual No. 1, rev. 2.2; Mitsubishi Heavy Industries, Tokyo, Japan 1992.
30. Wunderlich, B. J Therm Anal 1996, 46, 643.
31. Sperling, L. H. Introduction to Physical Polymer Science, 3rd ed.; Wiley-Intersience: New York, 2001; Chapter 8.